Received: 2 August 2021 | Revised: 13 June 2022 | Accepted: 28 June 2022

DOI: 10.1111/geb.13565

Global Ecology and Biogeography | WILEY

RESEARCH ARTICLE

Climatic and edaphic-based predictors of normalized difference vegetation index in tropical dry landscapes: A pantropical analysis

Marinés de la Peña-Domene[1] | Gerardo Rodríguez Tapia[1] | Natalia Mesa-Sierra[2] | Anaitzi Rivero-Villar[1] | Christian P. Giardina[3] | Nels G. Johnson[4] | Julio Campo[1]

[1]Instituto de Ecología, Universidad Nacional Autónoma de México, Mexico City, Mexico

[2]Instituto Tecnológico y de Estudios Superiores de Occidente, Centro Interdisciplinario para la Formación y Vinculación Social, Tlaquepaque, Mexico

[3]Institute of Pacific Islands Forestry, Pacific Southwest Research Station, USDA Forest Service, Hilo, Hawaii, USA

[4]USDA Forest Service, Pacific Southwest Research Station, Albany, California, USA

Correspondence
Julio Campo, Instituto de Ecolog a, Universidad Nacional Autónoma de México, Mexico City 04510, Mexico.
Email: jcampo@ecologia.unam.mx

Present address
Marinés de la Peña-Domene, Centro Interdisciplinario para la Formación y Vinculación Social, Instituto Tecnológico y de Estudios Superiores de Occidente, Tlaquepaque, Mexico

Handling Editor: Thomas Gillespie

Abstract

Aim: Spatial patterns in resource supply drive variability in vegetation structure and function, yet quantification of this variability for tropical dry forests (TDFs) remains rudimentary. Several climate-driven indices have been developed to classify and delineate TDFs globally, but there has not been a climo-edaphic synthesis of these indices to assess and delineate the extent of TDFs. A statistical climo-edaphic synthesis of these indices is therefore required.

Location: Pantropical.

Time period: Modern.

Major taxa studied: Vascular plants.

Methods: We assembled most known prior descriptions of TDFs into a single data layer and assessed statistically how the TDF biome, which we call tropical dry landscapes (TDLs) composed of forest and non-forest vegetation, varied with respect to the normalized difference vegetation index (NDVI) sensed by MODIS (250 m pixel resolution). We examined how the NDVI varied with respect to mean annual temperature (MAT) and rainfall (MAR), precipitation regime, evapotranspiration and the physical, chemical and biological properties of TDL soils.

Results: Overall, the NDVI varied widely across TDLs, and we were able to identify five principal NDVI categories. A regression tree model captured 90% of NDVI variation across TDLs, with 14 climate and soil metrics as predictors. The model was then pruned to use only the three strongest metrics. These included the Lang aridity index, total evapotranspiration (ET) and MAT, which aligned with identified NDVI thresholds and accounted for 70% of the variation in NDVI. We found that across a global TDL distribution, ET was the strongest positive predictor and MAT the strongest negative predictor of the NDVI.

Main conclusions: The remote sensing-based approach described here provides a comprehensive and quantitative biogeographical characterization of global TDL occurrence and the climatic and edaphic drivers of these landscapes.

KEYWORDS
climate, continental scale, MODIS, prediction, remote sensing, soil, tropical forest biome

1 | INTRODUCTION

The structure and function of tropical forests are strongly constrained by climatic and edaphic conditions, of which interannual and seasonal variation in rainfall and temperature and soil nutrient supply are viewed as being most important (Baldocchi et al., 2001; Ballantyne et al., 2017; Doughty et al., 2015; Green et al., 2019; Law et al., 2002; Litton & Giardina, 2008; Muller-Landau et al., 2021; Sullivan et al., 2020; Zhang et al., 2016; Zhao & Running, 2010). Spatial and temporal variation in rainfall is widely viewed as a central determinant of the occurrence of tropical dry forests (TDFs), with 3–10 months of annual drought characterizing the TDF biome (Chidumayo & Gumbo, 2010; FAO, 2012). The intra-annual amount and distribution of rainfall strongly modulate TDF structure and function, especially the carbon (C) cycle (Campo & Merino, 2016; Mendes et al., 2020; Rojas-Robles et al., 2020), with interannual variation in rainfall providing secondary controls (Allen et al., 2017; Huang et al., 2021). Additionally, the TDF biome is associated with high intensities of land use that create dynamic mosaics of forest, land under agricultural use and land supporting other human practices (Banda et al., 2016; Blackie et al., 2014). These uses often alter TDF composition, structure and function, and for this reason, we describe the TDF biome as comprising both forest and non-forest vegetation that together form tropical dry landscapes (TDLs). Given that TDF and savannas can co-occur in a range of environmental conditions (Moncrieff et al., 2015; Staver et al., 2011), large savanna matrices encompass patches of TDF in some TDLs, resulting in a mix of TDF and fire-dependent grass- and shrub-dominated ecosystems.

The strong sensitivity of TDLs to spatial and temporal variation in rainfall is reflected in the dominant indicators of TDFs and TDLs, including mean annual rainfall (MAR), mean annual temperature (MAT) and the number of sequential dry months in the dry season (Supporting Information Table S1). Typically, TDF is characterized by a MAT >17°C, an MAR range of 100–2,000 mm and an annual ratio of potential evapotranspiration (PET) to MAR that exceeds unity (Murphy & Lugo, 1986). The most important driver of TDF structure and function is pronounced intra-annual variation in the amount of rainfall, with each dry season month receiving <100 mm of rainfall (Pennington et al., 2009).

Spatial variation in plant primary production and associated C process rates are driven by climate and soil properties (Schlesinger & Bernhardt, 2020), and broad-scale relationships between climate and forest productivity reveal strong effects of moisture and temperature (Litton & Giardina, 2008; Luyssaert et al., 2007). In TDFs, the amount of dry season rainfall relative to atmospheric demand (i.e., the evapotranspiration that would be achieved from a well-aerated soil/plant surface at field water-holding capacity; Schwartz et al., 2020) appears to be a strong predictor of ecosystem productivity (Stan et al., 2021). Remote sensing is a central tool for monitoring C stocks and fluxes at regional to global scales (Cao et al., 2018; Ssemmanda et al., 2014), with the satellite-derived normalized difference vegetation index (NDVI) providing data at high temporal resolution for understanding the dynamics of vegetation greenness at the planetary scale. Particularly relevant for TDL analyses are the NDVI responses to MAT, MAR and both inter- and intra-annual climate variation (Linscheid et al., 2020; Pan et al., 2018; Walther et al., 2002; Yu et al., 2003; Zeng et al., 2013; Zhou et al., 2014). Globally, NDVI-based analyses reveal that warmer temperatures in combination with lower amounts of rainfall reduce greenness, hence productivity, with these relationships being strongest in low-latitude forests (Allen et al., 2010; Becknell et al., 2012). Finer-scale patterns within TDLs are less well understood, limiting efforts to model TDF responses to climate change accurately.

Here, we build on previous work (Corona-Núñez et al., 2018; Mallegowda et al., 2015) to examine how variation in climate and soils relates to NDVI across a global range of TDL sites. Specifically, we: (1) constructed a comprehensive database of published TDF ecoregions; (2) conducted spatial and temporal analyses of the relationships between NDVI and diverse climatic and edaphic variables for these ecoregions; and from this (3) established a generalized climo-edaphic statistical model to characterize global TDLs. To achieve these goals, we analysed 80 globally distributed and biogeographically defined TDF ecoregions. The specific objectives of this research were to: (1) evaluate how the variables most used to describe TDF are related to NDVI for previously identified TDLs in Afrotropical, Australasian, Indo-Malayan, Neotropical and Oceanian biogeographical regions; (2) use climatic and edaphic variables to assign TDLs to NDVI-based ecological groups; and (3) quantify how variation of these NDVI-based ecological groups relates to interannual climate variation.

2 | METHODS

2.1 | Categorization and selection of biogeographical regions and ecoregions

To characterize global variation in TDLs robustly, we identified five broad biogeographical regions where this ecosystem is distributed: Afrotropical, Australasian, Indo-Malayan, Neotropical and Oceanian. Each of these biogeographical regions is characterized by a physical environment (e.g., climate) and geological history that defines the ecosystem processes and prominent species distributions. Across these five regions, we identified 80 ecoregions based on three criteria that correspond to polygons generated by the World Wide Fund for Nature: (1) whether the site was identified as TDF by Olson et al. (2001) and revised by Dinerstein et al. (2017); (2) whether a site was described as TDF by authors who have focused their efforts and research on the description of this ecosystem within each of the five biogeographical regions (Supporting Information Table S1); and (3) whether sites were described as TDF in the FAO (2012) assessment of TDF (Figure 1) (Supporting Information Table S2). Unavoidably, we included disturbance-driven vegetation types, such as savanna, and geomorphologically determined vegetation types, such as riparian forests, which transition into adjacent TDFs that shape TDL dynamics (Dexter et al., 2018). To refine our understanding of

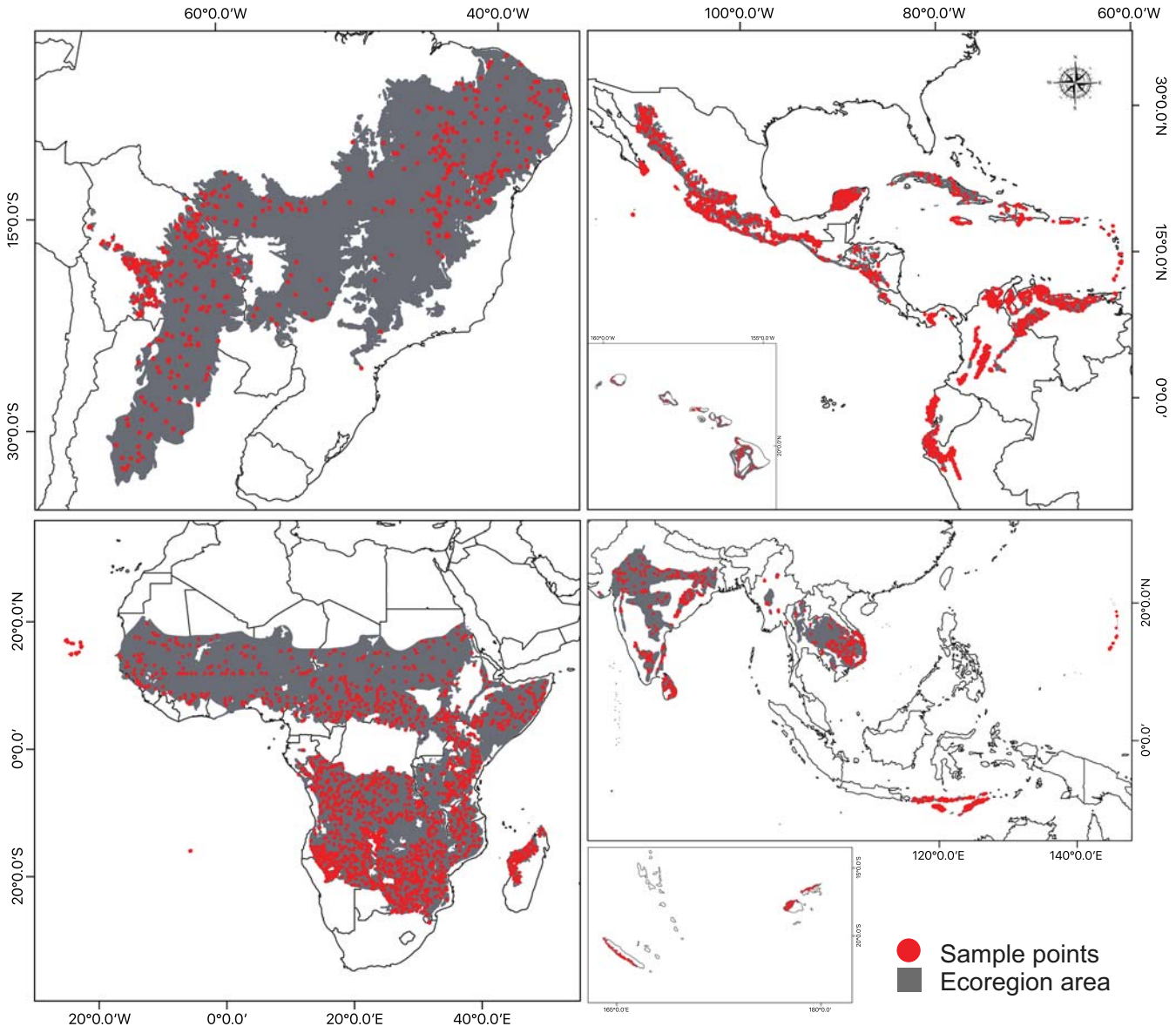

FIGURE 1 The distribution of tropical dry forest ecoregions (in grey) examined in this global synthesis. Red circles indicate the distribution of the 100 sample points within each ecoregion.

environmental controls on TDFs, we compiled diverse climatic and edaphic information with which to quantify variation in NDVI across the five major biogeographical regions and the 80 ecoregions. We excluded the following TDF types. Australia was excluded from the Australasian region because, for the scale of this analysis, it did not contain representative coverage of TDF. We also excluded a small island TDF from the Oceanic biogeographical region, Yap Tropical Dry Forests, because this ecoregion was missing data needed to assess NDVI.

2.2 | Selection of sample points

We created a 1 km^2 grid for each of the five biogeographical regions and identified the centroid of each cell of the grid, which we used as a sample point. We selected 100 sample points in a random block design from the full population of centroids for a given ecoregion and repeated this for each of the 80 studied ecoregions. We then used the HILDA+ Global Land Use Change layer (HILDAplus_vGLOB-1.0; Winkler et al., 2021) to evaluate the types of land use for the resulting grid of 8,000 points. The HILDA+ layer contains land cover information from 1960 to 2019, which allowed us to mask points defined as urban, cropland, ocean, water or as missing data. We used the remaining unmasked points, defined as forest, shrubland, pasture, rangeland or unmanaged grassland, in our analyses. These latter categories containing perennial TDL vegetation made up the 5,831 sample points used in our analyses. We used a randomized block design to assess relationships between NDVI and climatic and edaphic variations found across TDLs (Figure 1). All spatial analyses were conducted

in ArcGIS v.10.2.1. We assumed some level of homogeneity within a given ecoregion with respect to soils, climate, flora, fauna and other factors to examine ecological patterns across each of the 80 ecoregions (Dinerstein et al., 2017; Olson et al., 2001).

2.3 | Normalized difference vegetation index

We used 12 years (2005–2016) of NDVI data (250 m pixel resolution) collected with Moderate Resolution Imaging Spectroradiometer (MODIS) instruments aboard US National Aeronautics and Space Administration (NASA) Terra and Aqua satellites. The MODIS product was used because of its longevity, resolution and frequent observations. Data analyses relied on 12-year mean NDVI conditions for each of the 80 ecoregions sampled here. Although data are collected sub-weekly, we used averaged monthly data to calculate mean annual NDVI for the 12-year period. NDVI is dimensionless and ranges from −.1 to .9, with higher values being associated with denser vegetation and lower values associated with sparser vegetation. The lowest values represent bare ground.

2.4 | Climatic and edaphic metrics

For each sample point, we obtained rainfall, temperature and evapotranspiration data from repositories including: NASA Earth Observations (https://neo.gsfc.nasa.gov/); Climatic Hazards Center, UC Santa Barbara (www.chc.ucsb.edu/about); Numerical Terradynamic Simulation Group (NTSG), University of Montana (www.ntsg.umt.edu/); Oak Ridge National Laboratory Distributed Active Archive Center (ORNL DAAC) for Biogeochemical Dynamics (www.daac.ornl.gov/); and SOILGRID (www.soilgrids.org/). We examined a total of 17 climate variables: four temperature metrics, 10 precipitation metrics, an evapotranspiration metric and two aridity metrics that integrate annual precipitation and temperature measures (Table 1). All climate variables were summarized into mean annual averages representing between 1 and 12 years of available data (Supporting Information Table S3). We also considered 17 edaphic metrics involving physical, chemical and biological properties of soils (Table 1). These were all represented by a single point in time measurement and therefore have no temporal averaging component. Each of the 34 metrics was processed and normalized to standard units. Detailed information on the time frame, scale, units and reference sources for each of the 34 variables used are specified in the Supporting Information (Table S3).

2.5 | Data analyses

We explored mean annual NDVI variation against mean annual precipitation, number of dry months and mean annual temperature. We used multiple regression models to relate these metrics to NDVI. Our assessment was comprehensive with respect to global distribution of the TDF biome, but we did not evaluate the effects of forest successional age or ecological condition.

To identify and delineate different NDVI-based ecological groups within different biogeographical regions, we assumed that the mean NDVI value (mNDVI) for each observation, *i*, is represented by the following model:

$$\mathrm{mNDVI}_i = \mathrm{Normal}\left(\mu_i, \sigma^2\right),$$

$$\mu_i \approx f\left(\boldsymbol{x}_i\right),$$

where mean μ_i is well approximated by a regression tree (Breiman et al., 1984) function, *f*, of covariates $\boldsymbol{x}_i$, and the error variance is σ^2.

We used Pearson coefficients to identify significant climate and edaphic predictors of NDVI at both pantropical and biogeographical region scales. Bonferroni corrections were used whenever multiple pairwise comparisons were made. The *rpart* package (Therneau & Atkinson, 2019) in R v.3.6 computer programming language (R Core Team, 2019) was used to compute a regression tree with a maximum depth of 30. We performed 10-fold cross-validation to select the value of the complexity parameter that minimizes the cross-validation error. The complexity parameter penalizes the regression tree for adding further splits. See documentation of *rpart* for more details (Therneau & Atkinson, 2019). We repeated the 10-fold cross-validation 99 more times to compute a total of 100 values for the optimal complexity parameter. We then used the average of the 100 values as the optimal complexity parameter to prune the regression tree. This led to a tree with 137 splits and an r^2 of .90. We also pruned the regression tree so that the r^2 was reduced to .80, which led to a regression tree with 13 splits. Although this second tree is expected to have more biased predictions than the tree selected by cross-validation, it has the practical value of 13 splits being generally easier to interpret and discuss compared with 137 splits. Pruning the regression tree to an r^2 of .70 resulted in five splits, which we present and discuss below. Finally, using the NDVI differentiated ecological groups from the regression tree, multiple regressions were used to explore variation against principal components in analyses designed to capture edaphically or climatically driven variation in NDVI.

3 | RESULTS

3.1 | Tropical dry landscapes and NDVI distributions across ecoregions

The five biogeographical regions examined here contain 80 TDL ecoregions distributed across four continents (Figure 2). The Afrotropical biogeographical region represented 68% of global TDLs and contained 25 ecoregions, one of which accounted for 15% of all TDL (Sahelian Acacia Savanna). The Neotropical biogeographical region represented 24% of total TDL and contained 35 ecoregions. The Indo-Malayan, Australasian and Oceanian biogeographical regions combined to represent 8.4% of all TDL, with 20 ecoregions. We found considerable

TABLE 1 Normalized difference vegetation index (NDVI), climate and soil characteristics for the 80 tropical dry forest ecoregions studied

Characteristic	Metrics	Mean	CV (%)	Quartile (0.25)	Median	Quartile (0.75)
Vegetation						
1	Normalized difference vegetation index	0.58	28.8	0.46	0.61	0.70
Climate						
2	Mean annual temperature (°C)	28.6	13.2	25.9	28.2	39.3
3	Maximum temperature of the hottest month (°C)	34.4	16.9	29.7	34.3	39.3
4	Minimum temperature of the coldest month (°C)	24.1	12.4	22.5	24.1	25.6
5	Amplitude or range in temperature (°C)	10.3	48.2	6.3	9.9	14.5
6	Mean annual precipitation (mm)	1,118.1	55.2	662.1	1,060.6	1,504.6
7	Maximum precipitation in the wettest month (mm)	229.9	53.0	146.2	216.2	290.7
8	Minimum precipitation in the driest month (mm)	11.5	154.8	0.79	4.2	14.0
9	Amplitude or range in precipitation (mm)	218.4	54.9	135.8	203.2	276.2
10	Number of rainy months (>100 mm of precipitation per month)	4.5	59.2	3	5	6
11	Total precipitation in the rainy season (mm)	891.1	72.9	348.8	872.7	1,313.6
12	Concentration of precipitation in the rainy season (%)	67.5	45.1	54.8	81.6	89.2
13	Number of dry months (<100 mm of precipitation per month)	7.5	35.4	6	7	9
14	Number of months under hydric stress	4.5	66.5	2	5	7
15	Precipitation in the driest quarter of the year (mm)	51.8	146.9	5.8	23.0	70.7
16	Lang aridity index	41.0	61.7	22.2	37.6	55.3
17	Martonne aridity index	29.9	59.8	16.7	27.7	40.4
18	Mean annual evapotranspiration (mm)	883.4	45.7	553.5	888.2	1,214.2
Soil						
19	Depth (m)	2.1	62.3	1.3	1.9	3.6
20	Bulk density[a] (g/m^2)	1.4	9.6	1.4	1.5	1.5
21	Coarse fragments[a] (%)	13.2	75.4	6.0	11.0	18.0
22	Clay content[a] (%)	33.9	29.8	30.0	36.0	41.0
23	Field capacity[a] (mm)	408.2	10.2	390.5	412.9	429.9
24	Water-holding capacity[d] (mm)	354.0	52.6	234.0	330.0	418.0
25	Wilting point[a] (mm)	171.5	23.9	153.0	176.2	197.9
26	Potential storage of water from soil texture[d] (mm)	359.9	62.3	224.0	328.0	612.0
27	Potential storage of water in soil profile[d] (mm)	1,037.9	62.1	680.0	864.0	1,529.0
28	pH[a] (H_2O)	6.3	12.8	5.7	6.2	6.9
29	Cation exchange capacity[a,e] ($cmol_c/kg$)	17.6	40.8	12.3	17.5	21.7
30	Organic carbon[b] (Mg/ha)	59.2	115.1	26.1	37.8	57.9
31	Organic carbon[a,e] (Mg/ha)	75.6	92.8	35.5	56.8	81.5
32	Total nitrogen[a] (g/m^2)	919.2	67.3	345.6	919.0	1,364.7
33	Total phosphorus[c,f] (g/m^2)	430.9	71.1	272.4	321.9	503.8
34	Organic phosphorus[c,f] (g/m^2)	99.2	103.1	41.9	67.6	130.9
35	Labile inorganic phosphorus[c,f] (g/m^2)	40.1	87.9	19.7	34.7	42.5

Note: For each metric, standardized units are presented, in addition to the 25 and 75% quartiles for each metric. J

[a]Soil depth 0–1.0 m. J

[b]Soil depth 0–0.3 m. J

[c]Soil depth 0–0.5 m. J

[d]Soil depth not indicated. J

[e]This information was calculated using data of 0–0.05, 0.05–0.15, 0.15–0.30, 0.30–0.60 and 0.60–1.0 m soil layers in the case of cation exchange capacity and data of 0–0.30 and 0.30–1.0 m soil layers in the case of organic carbon. J

[f]This information needs to be interpreted with caution, because the values included are very large considering the values of nitrogen. J

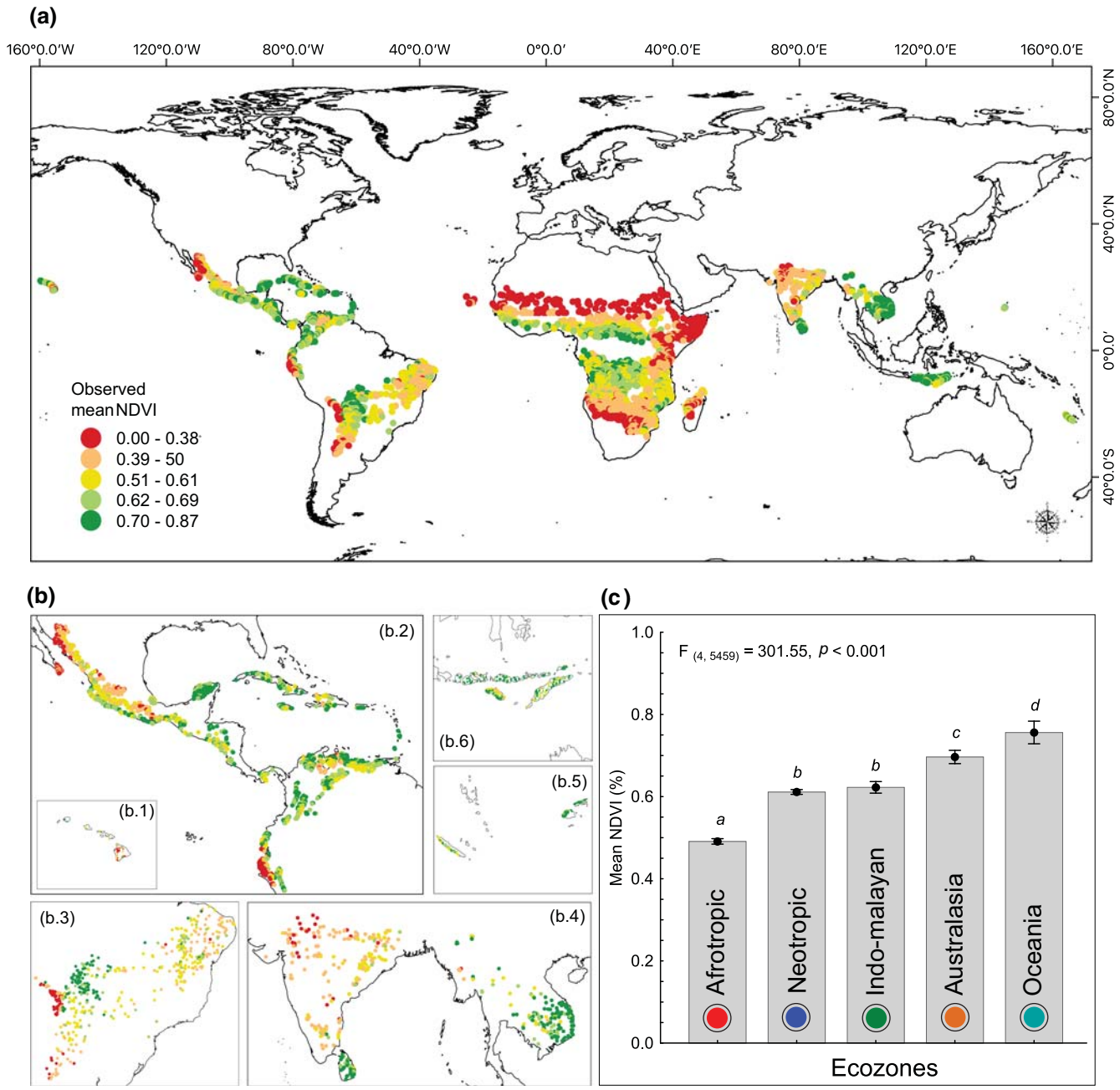

FIGURE 2 (a) Distribution of the normalized difference vegetation index (NDVI) across the biogeographical regions, with (b) high-resolution insets for: (b.1) Hawaiin islands, (b.2) Mexican and Central American and Antilles islands, (b.3) South America, (b.4) Indian and Thailand region, (b.5) Melanesian islands and (b.6) Indonesian islands. (c) Mean and standard error of NDVI for each biogeographical region. Circles indicate the means, the spreads denote 95% confidence intervals, and different letters indicate significant differences ($p < .05$) among biogeographical regions.

variation in average NDVI values across biogeographical regions, with mean values increasing as follows: Afrotropical < Indo-Malayan < Neotropical < Australasia < Oceania (Figure 2).

3.2 | Variation of climatic and edaphic metrics

The classic TDF metrics of MAT, MAR and mean annual number of dry months were important predictors of mean annual NDVI across the 5,831 TDL sample points and showed high variation across biogeographical regions (Table 1). MAT varied from 25.9 to 39.3°C, MAR varied from 662 to 1,505 mm, and the number of dry months varied between six and nine. Likewise, our two drought intensity metrics were highly variable, with mean minimum precipitation in the driest month ranging from <1 to 14 mm, and total precipitation in the driest quarter ranging from 6 to 71 mm (Table 1). We found that mean annual evapotranspiration (ET_m) varied from 554 to 1214 mm/year, and the coefficient of variation

(CV) for the Lang and Martonne aridity indices was nearly 60% (Table 1). Global-scale variation in physical soil properties was low for bulk density (CV = 9.6%) but high for potential water storage (CV = 62.3%). For soil chemical properties, pH varied from 5.7 to 6.9. For soil biological properties, organic carbon storage ranged from 26.1 to 57.9 Mg/ha (0–1.0 m in depth) while total phosphorus concentrations ranged from 272 to 504 g/m^2 (0–0.5 m in depth) (Table 1).

3.3 | Relationships of NDVI to climate and edaphic metrics

Pearson correlation analysis indicated that mean annual NDVI was strongly correlated with all 11 climatic metrics ($p < .001$), and these relationships were stronger than those with soil metrics (Supporting Information Table S4). The NDVI relationships with MAT, Lang aridity index, ET and the number of months under hydric stress were particularly strong, indicating a robust basis for using these four climate metrics as primary TDL indicators (Figure 3). The strength of the NDVI relationship with the 13 soil metrics was more variable, ranging from $r = -0.60$ in the case of pH ($p < .001$) to a non-significant relationship with total phosphorus content ($r = -0.02$, $p > .05$). We also observed differences in NDVI among biogeographical regions (Figure 2b) with the strength and number of significant metrics (Supporting Information Table S4).

We observed strong negative correlations between mean annual NDVI and the mean annual number of months under hydric stress ($r = -0.73$), mean temperatures in the warmest month ($r = -0.70$) and the mean number of the dry months ($r = -0.64$). Conversely, we observed strong positive correlations between NDVI and MAR ($r = 0.71$), mean rainfall in the wettest month ($r = 0.51$), mean total rainfall during the rainy season ($r = 0.60$), mean total rainfall in the driest quarter ($r = 0.42$) and mean rainfall in the driest month ($r = 0.40$) (Supporting Information Figure S1). The number of dry months also had a negative relationship with NDVI, with the highest NDVI values being associated with 2–4 months of drought, whereas the lowest NDVI values were associated with the highest number of dry months (Supporting Information Figure S1). The highest NDVI values were correlated with the highest ET_m values, whereas the lowest NDVI values were associated with the lowest MAP values (Supporting Information Figure S1). Of the edaphic metrics, pH was the best predictor of NDVI ($r = -0.60$), whereas water-holding capacity and field capacity were the best physical predictors of NDVI ($r = 0.38$ and 0.31, respectively; Supporting Information Figure S2). Soil organic carbon was the best but a somewhat weak biological predictor of NDVI ($r = 0.25$; Supporting Information Figure S3).

3.4 | Tropical dry landscape classification model

Our regression tree statistical modelling identified 14 climate and soil metrics as the most important predictors of NDVI variation across TDL (capturing 90% of variation; Figure 4a). This regression tree was pruned to reduce the number of splits, with only three variables needed to capture 70% of the variation in NDVI. This most parsimonious regression tree model included three climatic metrics (ET, Lang aridity index and MAT), which we used to partition our global TDL dataset into five NDVI-based ecological groupings (Figure 4b). The TDL with the highest NDVI value (group 5; Figure 4b) included sites with an ET_m of >989 mm. The number of months under hydric stress and the maximum temperature of the hottest month also had high importance values within the statistical model (Figure 4a). The lowest NDVI groups were located mainly in the Afrotropical biogeographical region, and the highest were in the Neotropical and Indo-Malayan biogeographical regions (Figure 4c). These analyses provide a quantitative global characterization that refines our understanding of the variability of this biome across spatial scales (Supporting Information Table S1).

4 | DISCUSSION

4.1 | What are tropical dry landscapes?

Mooney et al. (1995) identified TDFs as those forests occurring in tropical regions characterized by pronounced seasonality in the distribution of precipitation. Others have elaborated on the conditions required to sustain TDFs, including the role of MAP, MAT and the number of dry months (Supporting Information Table S1). To assess these classical relationships, we systematically characterized the climatically and edaphically driven spatial variation in TDL NDVI. Specifically, by inventorying a global distribution of 5,831 TDL sites and analysing how NDVI for these sites was correlated with 34 climatic and edaphic variables in regression tree analyses, we have developed a comprehensive statistical model for describing variation in global TDLs. This model includes three climatic metrics: ET, Lang aridity index and MAT. This model represents a parsimonious and robust improvement over classic single-index-based approaches to explaining ecoregional-scale variation in NDVI across TDLs.

We found that ET, Lang aridity index and MAT were sufficient to delineate global TDLs into five major NDVI categories, providing a novel climatic categorization of this forest into distinct biogeographical TDL types defined by NDVI, which is a remotely sensed attribute strongly linked to forest structure and function. The underlying climate relationships with NDVI indicate strong spatial variability in TDL structure and productivity across biogeographical regions and ecoregions. To this end, our five-tier categorization of TDL provides a structurally and functionally quantitative way to describe its global variation. Taken together, these findings highlight the value of a remote sensing-based statistical modelling approach to quantifying the extent and variation of the TDF biome. The climatic and edaphic variables used in the full model explained 90% of NDVI variation across TDLs. Moreover, although the pruned fitted regression tree model identified MAT, ET_m and Lang aridity index as important predictors of NDVI, explaining 70% of NDVI variation, neither ET_m nor

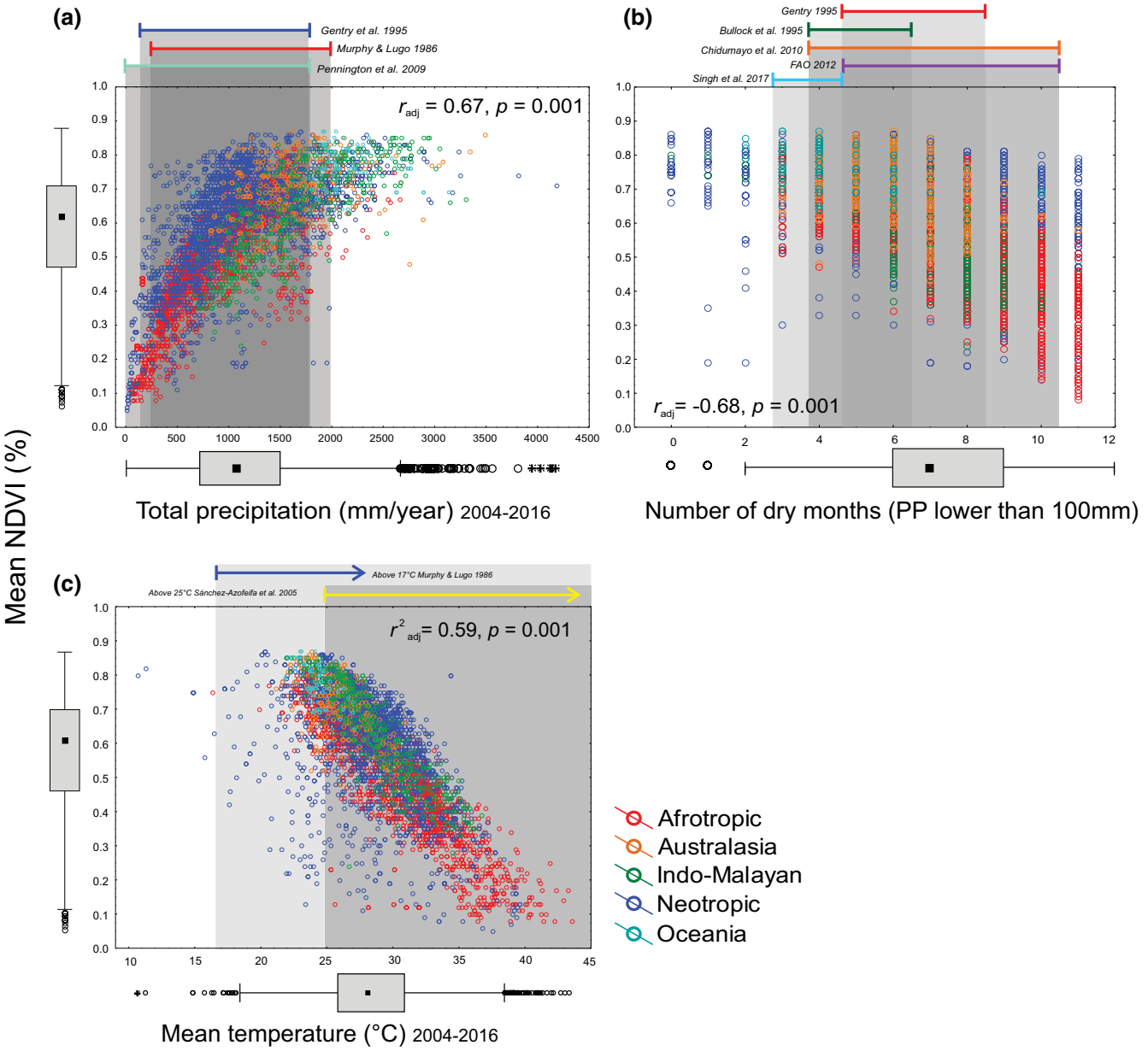

FIGURE 3 Relationships between normalized difference vegetation index (NDVI) and (a) mean annual precipitation, (b) number of dry months (precipitation <100 mm per month) and (c) mean annual temperature. Different colours represent the five different biogeographical regions. Grey shaded blocks identify regions of a figure defined as tropical dry forest by the authors listed above each panel (detailed in Supporting Information Table S1). Box plots show the median and standard deviation for each metric, with circles representing outliers and asterisks representing extreme values.

Lang aridity index has been used previously to characterize TDF biogeography.

4.2 | NDVI of tropical dry landscapes

Our statistical model relied on 34 climatic and edaphic characteristics to describe NDVI of the TDLs inventoried here. We used NDVI as an index of ecosystem productivity to delineate five types of TDLs. NDVI is easily accessible through GIS and provides the longest temporal record of global vegetation conditions, which allows for analyses of interannual variation, baseline climate change or the impact of specific events (Schloss et al., 1999). Generally, mean NDVI varies widely among TDL biogeographical regions, with more sensitivity to spatial variation in climate (positive relationship with ET_m and MAP; negative relationship with MAT) than with soils. These analyses suggest that TDL productivity is significantly constrained by the energy demand as defined by ET and by water supply as defined by MAR; the Budyko effect (Zhou et al., 2015). The effects of ET_m and precipitation on NDVI observed in our study align with findings that global C fluxes in water-limited regions are controlled primarily by precipitation and

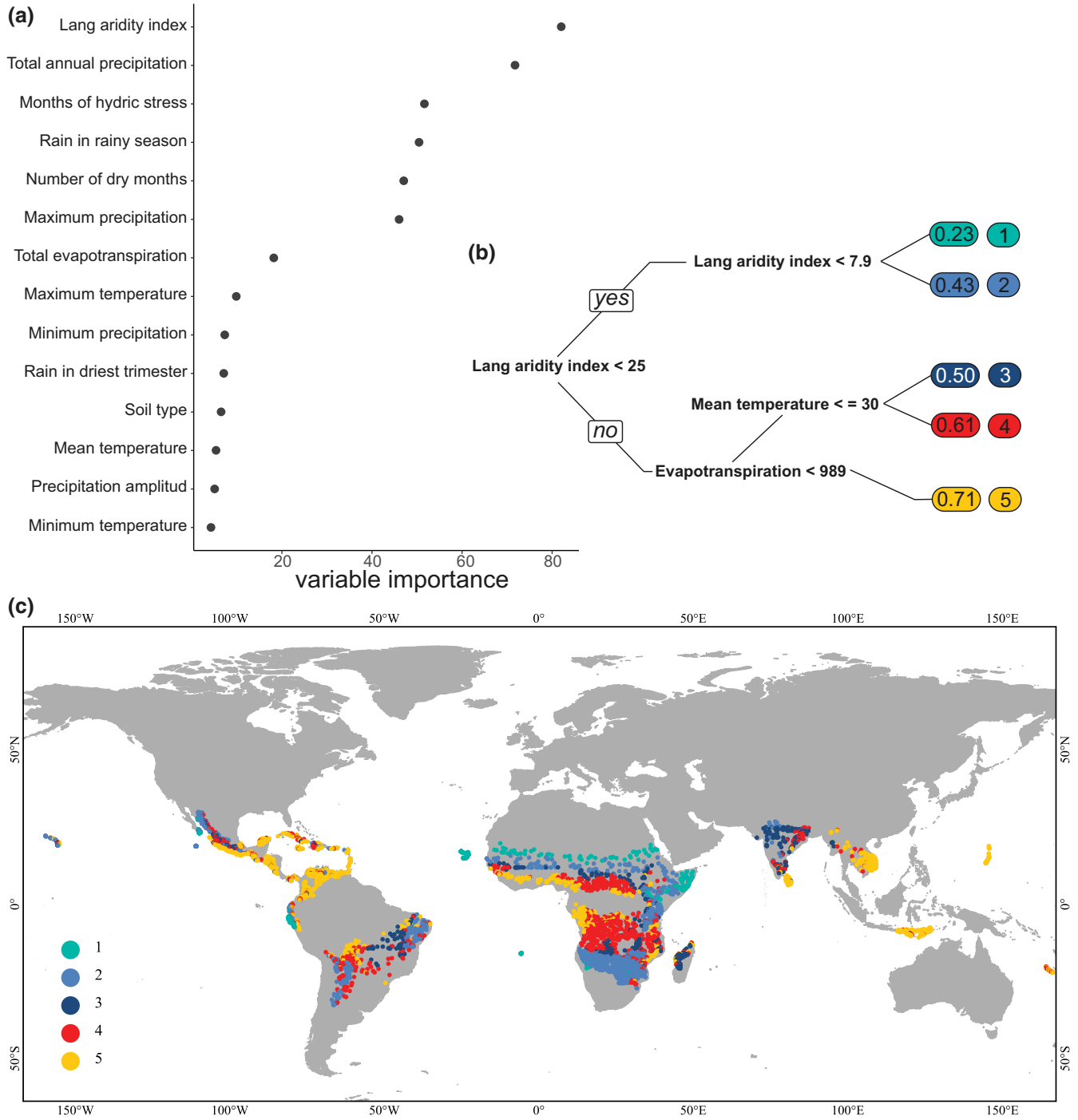

FIGURE 4 (a) Classification of the tropical dry landscapes analysed for the 80 tropical dry forest ecoregions. (b) Importance of climate and soil metrics within the regression tree decision model. (c) Map of the five identified normalized difference vegetation index-based regression tree-delineated tropical dry landscape groups.

ET (Poulter et al., 2014; Zhang et al., 2016). Our results show the strong coupling of NDVI to spatial variations in water availability in TDLs, including water-holding capacity of soils, at both global and regional scales, which aligns with the fast temporal response of vegetation to changes in water deficit in intensely water-limited environments (Becknell et al., 2012; Giraldo & Holbrook, 2011; Portillo-Quintero et al., 2015; Rojas-Robles et al., 2020; Vicente-Serrano et al., 2013), including seasonal moisture controls on ecosystem biogeochemistry (Castro et al., 2018; Liu et al., 2018; Mendes et al., 2020). Our findings are consistent with the broadly appreciated control that air temperature and precipitation via soil moisture have on plant growth and TDF dynamics (Green et al., 2019; Humphrey et al., 2018; Liu et al., 2018; Nemani, 2003; Seddon et al., 2016; Stan et al., 2021).

Conversely, because temperature is rarely limiting to canopy processes in the tropics (Huang et al., 2019), negative correlations with

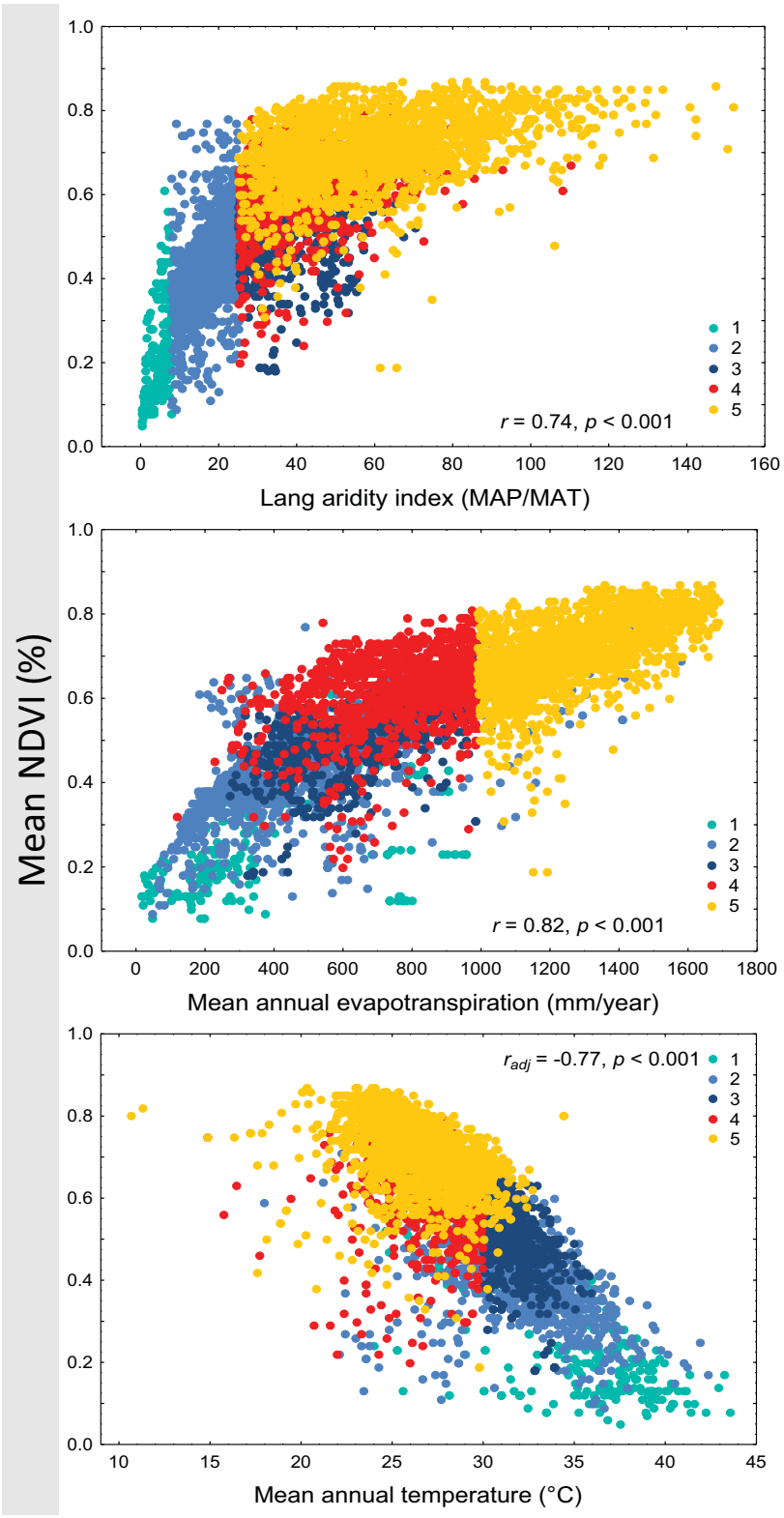

FIGURE 5 Relationships between normalized difference vegetation index (NDVI) and (a) Lang aridity index [ratio of mean annual precipitation (MAP) to mean annual temperature (MAT)], (b) mean annual evapotranspiration and (c) mean annual temperature. Different colours represent the five NDVI-based regression tree-delineated tropical dry landscape groups (see Figure 4).

MAT are expected. Given that NDVI saturates over regions of dense vegetation (Jones & Vaughan, 2010), results in the tropics need to be interpreted with caution (Linscheid et al., 2020). Across tropical dry, moist and wet forests, NDVI shows correlations with climate that vary within and across continents (Linscheid et al., 2020). Such spatial variation can be explained by the spatial variation in the strength of intra-annual seasonality of tropical environments, for example alterations in precipitation and temperature regimes associated with the Madden–Julian Oscillation (Zhang, 2005, 2013), which could drive temporal NDVI oscillations in the tropics (Hidayat, 2016; Mayta et al., 2019; Wang et al., 2019). Considering the long-term decrease in the amount of precipitation that is expected in seasonally dry tropical

regions (Chadwick et al., 2015; Greve et al., 2014; Huang et al., 2016), further investigation is needed on additional climatic factors (e.g., radiation) that might also exert a strong influence on C cycling in tropical forests (Lyu et al., 2021; Nemani, 2003; Seddon et al., 2016).

Our study explores how productivity is regulated in TDLs, with spatial variation being modestly dependent on soil properties. Soil pH consistently had a strong negative relationship with NDVI across ecoregions, probably reflecting the influence of soil fertility on productivity (Castro et al., 2018; Corona-Núñez et al., 2018; Hofhansl et al., 2020). Although there is evidence that productivity in TDFs can be phosphorus limited (Gei & Powers, 2014), our analyses of total soil phosphorus concentrations, a proxy for plant available phosphorus, show statistically non-significant relationships with mean annual NDVI across our 80 ecoregions. We cannot determine whether this pattern was driven by the negative relationship between NDVI and total soil phosphorus across Afrotropical and Indo-Malayan ecoregions or whether a positive real effect of this nutrient on NDVI was obscured by the stronger influence of ET_m and MAP on NDVI, with higher MAP, for example, driving lower phosphorus through enhanced weathering of soils.

4.3 | NDVI, biogeographical patterns and climate change

We found strong biogeographical patterns with respect to the NDVI groups at the pantropical scale. The lowest NDVI group (group 1) was located mainly in the Afrotropical biogeographical region, whereas the highest NDVI group (group 5) was located mainly in the Neotropical and Indo-Malayan biogeographical regions. Despite this geographical segregation, all five groups occurred in all three biogeographical regions. This overlap between NDVI groups within continents could reflect comparable variability in climatic and edaphic factors within biogeographical regions. Conversely, the overlap could relate to the lack of floristic differences between Africa and Asia, with floristic differences for the TDLs of the Neotropics (Dexter et al., 2015). Future research could focus whether TDL flora share a common biogeographical origin (Slik et al., 2018), whereby selection for drought and fire resistance has favoured the dominance of similar plant lineages globally (Banda et al., 2016; Ratnam et al., 2016).

Our pruned climo-edaphic regression tree model relied on MAT, ET_m and Lang aridity index, which we used to identify five global NDVI categories of TDLs and to highlight the structural and functional diversity of TDLs (Figure 4b). We also suggest that these delineations might represent thresholds that can be used to identify which categories of TDLs might be the most susceptible to climate change. For example, TDLs in the group 5 category show the highest NDVI values and support the highest ET_m and the lowest Lang Aridity Index values (Figure 5a,b) and might therefore represent areas that are less sensitive to warming and drying. Some group 5 category areas support TDF ecosystems that have resilience to both the high interannual droughts and the frequent within-rainy season droughts (Maass et al., 2018) and to high temperatures (González et al., 2018). In contrast, group 1 areas with the lowest NDVI values and highest MAT (Figure 5c) might occur at the climatic margins of the TDF biome. For example, ET_m differentiated the group with the highest NDVI values (group 5), whereas the Lang aridity index differentiated the two groups with the lowest NDVI values (groups 1 and 2). For group 1 areas found mainly in ecoregions of Africa and Neotropics of Brazil, MAR is very low and Lang aridity index very high, which affect plant growth negatively (D'Onofrio et al., 2018). When tree species diversity is high, TDF areas exhibit drought tolerance except in the most extreme circumstances (Stan & Sánchez-Azofeifa, 2019). When paired with climate change projections for an ecoregion or a biogeographical region, these delineations can be used to assess the potential for rapid change, including proximity to ecological tipping points (Scheffer et al., 2009). The existence of climate-driven thresholds has been suggested for diverse terrestrial ecosystems, including tropical rain forests (Lenton et al., 2008), but the nature of tipping points for TDFs is poorly understood (Lenton et al., 2008; Seddon et al., 2016; but see also Campo, 2016).

5 | CONCLUSIONS

We report here an improved approach to characterizing the TDF biome and address a long-standing question regarding climatic and edaphic controls on TDF distribution and function. This work advances a remote sensing-based analysis to characterize previously under-appreciated controls on the functioning of the TDF biome, with the 34 climatic and edaphic variables considered here explaining 90% of NDVI variation across TDLs. Furthermore, we report that the Lang aridity index, MAT and ET_m explain 70% of the variation in NDVI for this remarkably diverse biome. Our analysis points to a need to explore how the quantitative insights into NDVI variability can be used to anticipate susceptibility of the TDF biome to climate change. Our delineation of TDLs into five NDVI-based categories might prove useful in forecasting the ecosystem changes in response to climate change, especially declines in precipitation or increases in temperature.

AUTHOR CONTRIBUTIONS

M.P.-D., C.P.G. and J.C. designed the study. M.P.-D., G.R.T. and J.C. compiled the data. M.P.-D., N.M.-S., A.R.-V., C.P.G. and N.G.J. carried out the data analysis. M.P.-D., C.P.G. and J.C. led the writing, with input from all authors.

FUNDING INFORMATION

This work was supported by USDA Forest Service grant 17-IJ-l1272136 045.

DATA AVAILABILITY STATEMENT

The data that support the findings of this study are available at: "Tropical Dry Forest climatic edaphic and vegetation Database", Mendeley Data, V1, doi: 10.17632/6cx6k6k4yn.1.

ORCID

Julio Campo https://orcid.org/0000-0002-7595-8593

REFERENCES

Allen, C. D., Macalady, A., Chenchouni, H., Bachelet, D., McDowell, N., Vennetier, M., Kitzberger, T., Rigling, A., Breshears, D. D., Hogg, E. H. T., Gonzalez, P., Fensham, R., Zhang, Z., Castro, J., Demidova, N., Lim, J.-H., Allard, G., Running, S. W., Semerci, A., & Cob, N. (2010). A global overview of drought and heat-induced tree mortality reveals emerging climate change risks for forests. *Forest Ecology and Management*, *259*, 660–684.

Allen, K., Dupuy, J. M., Gei, M. G., Hulshof, C., Medvigy, D., Pizano, C., Salgado-Negret, B., Smith, C. M., Trierweiler, A., Van Bloem, S. J., Waring, B. G., Xu, X., & Powers, J. S. (2017). Will seasonally dry tropical forests be sensitive or resistant to future changes in rainfall regimes? *Environmental Research Letters*, *12*, 023001.

Baldocchi, D. D., Falge, E., Gu, L., Olson, R., Hollinger, D. Y., Running, S. W., Anthoni, P., Bernhofer, C., Davis, K., Evans, R., Fuentes, J., Goldstein, A., Katul, G., Law, B., Lee, X., Malhi, Y., Meyers, T., Munger, W., Oechel, W., … Wofsy, S. (2001). FLUXNET: A new tool to study the temporal and spatial variability of ecosystem scale carbon dioxide, water vapor, and energy flux densities. *Bulletin of the American Meteorological Society*, *82*, 2415–2434.

Ballantyne, A., Smith, W., Anderegg, W., Kauppi, P., Sarmiento, J., Tans, P., Shevliakova, E., Pan, Y., Poulter, B., Anav, A., Friedlingstein, P., Houghton, R., & Running, S. (2017). Accelerating net terrestrial carbon uptake during the warming hiatus due to reduced respiration. *Nature Climate Change*, *7*, 148–152.

Banda, R. K., Delgado-Salinas, A., Dexter, K. G., Linares-Palomino, R., Oliveira-Filho, A., Prado, D., Pullan, M., Quintana, C., Riina, R., Rodr guez, G. M., Weintritt, J., Acevedo-Rodr guez, P., Adarve, J., Álvarez, E., Aranguren, A. B., Arteaga, J. C., Aymard, G., Castaño, A., Ceballos-Mago, N., … Pennington, R. T. (2016). Plant diversity patterns in neotropical dry forests and their conservation implications. *Science*, *353*, 1383–1387.

Becknell, J. M., Kucek, L. K., & Powers, J. S. (2012). Aboveground biomass in mature and secondary seasonally dry tropical forests: A literature review and global synthesis. *Forest Ecology and Management*, *276*, 88–95.

Blackie, R., Baldauf, C., Gautier, D., Gumbo, D., Kassa, H., Parthasarathy, N., Paumgarten, F., Sola, P., Pulla, S., Waeber, P., & Sunderland, T. C. H. (2014). *Tropical dry forests: The state of global knowledge and recommendations for future research*. Center for International Forestry Research.

Breiman, L., Friedman, J., Olshen, R., & Stone, C. (1984). *Classification and regression trees*. Wadsworth International Group.

Campo, J. (2016). Shift from ecosystem P to N limitation at precipitation gradient in dry tropical forests at Yucatan, Mexico. *Environmental Research Letters*, *11*, 095006.

Campo, J., & Merino, A. (2016). Variations in soil carbon sequestration and their determinants along a precipitation gradient in seasonally dry tropical forests. *Global Change Biology*, *22*, 1942–1956.

Cao, Z., Li, Y., Liu, Y., Chen, Y., & Wang, Y. (2018). When and where did the loess plateau turn "green"? Analysis of the tendency and breakpoints of the normalized difference vegetation index. *Land Degradation & Development*, *29*, 162–175.

Castro, S. M., Sánchez-Azofeifa, G. A., & Sato, H. (2018). Effect of drought on productivity in aCosta Rican tropical dry forest. *Environmental Research Letters*, *13*, 045001.

Chadwick, R., Good, P., Martin, G., & Rowell, D. P. (2015). Large rainfall changes consistently projected over substantial areas of tropical land. *Nature Climate Change*, *6*, 177–181.

Chidumayo, E. N., & Gumbo, D. J. (2010). *The dry forests and woodlands of Africa: Managing for products and services*. Routledge.

Corona-Núñez, R. O., Campo, J., & Williams, M. (2018). Aboveground carbon storage in tropical dry forest plots in Oaxaca, Mexico. *Forest Ecology and Management*, *409*, 202–214.

Dexter, K. G., Pennington, R. T., Oliveira-Filho, A. T., Bueno, M. L., Silva de Miranda, P. L., & Neves, D. M. (2018). Inserting tropical dry forests into the discussion on biome transitions in the tropics. *Frontiers in Ecology and Evolution*, *6*, 104.

Dexter, K. G., Smart, B., Baldauf, C., Baker, T. R., Balinga, M. P., Brienen, R. J. W., Fauset, S., Feldpausch, T. R., Silva, L. F.-D., Muledi, J. I., Lewis, S. L., Lopez-Gonzalez, G., Marimon-Junior, B. H., Marimon, B. S., Meerts, P., Page, N., Parthasarathy, N., Phillips, O. L., Sunderland, T. C. H., … Pennington, R. T. (2015). Floristics and biogeography of vegetation in seasonally dry tropical regions. *International Forest Review*, *17*, 10–22.

Dinerstein, E., Olson, D., Joshi, A., Vynne, C., Burgess, N. D., Wikramanayake, E., Hahn, N., Palminteri, S., Hedao, P., Noss, R., Hansen, M., Locke, H., Ellis, E. C., Jones, B. S., Barber, C. V., Hayes, R., Kormos, C., Martin, V., Crist, E., … Saleem, M. (2017). An ecoregion-based approach to protecting half the terrestrial realm. *Bioscience*, *67*, 534–545.

D'Onofrio, D., von Hardenberg, J., & Baudena, M. (2018). Not only trees: Grasses determine African tropical biome distributions via water limitation and fire. *Global Ecology and Biogeography*, *27*, 714–725.

Doughty, C. E., Metcalfe, D. B., Girardin, C. A. J., Farfán Amézquita, F., Galiano Cabrera, D., Huaraca Huasco, W., Silva-Espejo, J. E., Araujo-Murakami, A., da Costa, M. C., Rocha, W., Feldpausch, T. R., Mendoza, A. L. M., da Costa, A. C. L., Meir, P., Phillips, O. L., & Malhi, I. (2015). Drought impact on forest carbon dynamics and fluxes in Amazonia. *Nature*, *519*, 78–82.

FAO. (2012). *Global ecological zones for FAO forest reporting: 2010 update*. Food and Agriculture Organization of the United Nations.

Gei, M. G., & Powers, J. S. (2014). Nutrient cycling in tropical dry forests. In A. Sánchez-Azofeifa, J. S. Powers, G. W. Fernandes, & M. Quesada (Eds.), *Tropical dry forests in the Americas: Ecology, conservation, and management* (pp. 141–154). CRC Press.

Giraldo, J. P., & Holbrook, N. M. (2011). Physiological mechanisms underlying the seasonality of leaf senescence and renewal in seasonally dry tropical forest trees. In R. Dirzo, H. S. Young, H. A. Mooney, & G. Ceballos (Eds.), *Seasonally dry tropical forests: Ecology and conservation* (pp. 129–140). Island Press.

González, M. R., Garc a, H., Isaacs, P., Cuadros, H., López-Camacho, R., Rodr guez, N., Pérez, K., Mijares, F., Castaño-Naranjo, A., Jurado, R., Idárraga-Piedrah ta, Á., Rojas, A., Vergara, H., & Pizano, C. (2018). Disentangling the environmental heterogeneity, floristic distinctiveness and current threats of tropical dry forests in Colombia. *Environmental Research Letters*, *13*, 045007.

Green, J. K., Seneviratne, S. I., Berg, A. M., Findell, K. L., Hagemann, S., Lawrence, D. M., & Gentine, P. (2019). Large influence of soil moisture on long-term terrestrial carbon uptake. *Nature*, *565*, 476–479.

Greve, P., Orlowsky, B., Mueller, B., Sheffield, J., Reichstein, M., & Seneviratne, S. I. (2014). Global assessment of trends in wetting and drying over land. *Nature Geoscience*, *7*, 716–721.

Hidayat, R. (2016). Modulation of Indonesian rainfall variability by the madden–Julian oscillation. *Procedia Environmental Sciences*, *33*, 167–177.

Hofhansl, F., Chacón-Madrigal, E., Fuchslueger, L., Jenking, D., Morera-Beita, A., Plutzar, C., Silla, F., Andersen, K. M., Buchs, D. M., Dullinger, S., Fiedler, K., Franklin, O., Hietz, P., Huber, W., Quesada, C. A., Rammig, A., Schrodt, F., Vincent, A. G., Weissenhofer, A., & Wanek, W. (2020). Climatic and edaphic controls over tropical diversity and vegetation carbon storage. *Scientific Reports*, *10*, 5066.

Huang, C.-Y., Durán, S. M., Hu, K.-T., Li, H.-J., Swenson, N. G., & Enquist, B. J. (2021). Remotely sensed assessment of increasing chronic

and episodic drought effects on aCosta Rican tropical dry forest. *Ecosphere*, *12*, e03824.

Huang, J., Yu, H., Guan, X., Wang, G., & Guo, R. (2016). Accelerated dryland expansion under climate change. *Nature Climate Change*, *6*, 166–171.

Huang, M., Piao, S., Ciais, P., Peñuelas, J., Wang, X., Keenan, T. F., Peng, S., Berry, J. A., Wang, K., Mao, J., Alkama, R., Cescatti, A., Cuntz, M., De Deurwaerder, H., Gao, M., He, Y., Liu, Y., Luo, Y., Myneni, R. B., … Janssens, I. A. (2019). Air temperature optima of vegetation productivity across global biomes. *Nature Ecology and Evolution*, *3*, 772–779.

Humphrey, V., Zscheischler, J., Ciais, P., Gudmundsson, L., Sitch, S., & Seneviratne, S. I. (2018). Sensitivity of atmospheric CO_2 growth rate to observed changes in terrestrial water storage. *Nature*, *560*, 628–631.

Jones, H. G., & Vaughan, R. A. (2010). *Remote sensing of vegetation: Principles, techniques, and applications*. Oxford University Press.

Law, B. T., Falge, E., Gu, L., Baldocchi, D. D., Bakwin, P., Berbigier, P., Davis, K. J., Dolman, A. J., Falk, M., Fuentes, J. D., Goldstein, A. H., Granier, A., Grelle, A., Hollinger, D. Y., Janssens, I. A., Jarvis, P., Jensen, N. O., Katul, G., Mahli, Y., … Wofsy, S. (2002). Environmental controls over carbon dioxide and water vapor exchange of terrestrial vegetation. *Agricultural and Forest Meteorology*, *113*, 97–120.

Lenton, T. M., Held, H., Kriegler, E., Hall, J. W., Lucht, W., Rahms, S., & Schellnhuber, H. J. (2008). Tipping elements in the Earth's climate system. *Proceedings of the National Academy of Science of the USA*, *105*, 1786–1793.

Linscheid, N., Estupinan-Suarez, L. M., Brenning, A., Carvalhais, N., Cremer, F., & Gans, F. (2020). Towards a global understanding of vegetation-climate dynamics at multiple timescales. *Biogeosciences*, *17*, 945–962.

Litton, C. M., & Giardina, C. P. (2008). Below-ground carbon flux and partitioning: Global patterns and response to temperature. *Functional Ecology*, *22*, 941–954.

Liu, L., Zhang, Y., Wu, S., Li, S., & Qin, D. (2018). Water memory effects and their impacts on global vegetation productivity and resilience. *Scientific Reports*, *8*, 2962.

Luyssaert, S., Inglima, I., Jung, M., Richardson, A. D., Reichstein, M., Papale, D., Piao, S. L., Schulzes, E. D., Wingate, L., Matteucci, G., Aragao, L., Aubinet, M., Beers, C., Bernhoffer, C., Black, K. G., Bonal, D., Bonnefond, J. M., Chambers, J., Ciais, P., ..Janssens, I. A. (2007). CO_2 balance of boreal, temperate, and tropical forests derived from a global database. *Global Change Biology*, *13*, 2509–2537.

Lyu, M., Giardina, C. P., & Litton, C. M. (2021). Interannual variation in rainfall modulates temperature sensitivity of carbon allocation and flux in a tropical montane wet forest. *Global Change Biology*, *27*, 3824–3836.

Maass, M., Ahedo-Hernández, R., Araiza, S., Verduzco, A., Mart nez-Yr zar, A., Jaramillo, V. J., Parker, G., Pascual, F., Garc a-Méndez, G., & Sarukhán, J. (2018). Long-term (33 years) rainfall and runoff dynamics in a tropical dry forest ecosystem in western Mexico: Management implications under extreme hydrometeorological events. *Forest Ecology and Management*, *426*, 7–17.

Mallegowda, P., Rengaian, G., Krishnan, J., & Niphadkar, M. (2015). Assessing habitat quality of forest-corridors through NDVI analysis in dry tropical forests of South India: Implications for conservation. *Remote Sensing*, *7*, 1619–1639.

Mayta, V. C., Ambrizzi, T., Espinoza, J. C., & Dias, P. L. S. (2019). The role of the madden-Julian oscillation on the Amazon basin intraseasonal rainfall variability. *International Journal of Climatology*, *39*, 343–360.

Mendes, K. R., Campos, S., da Silva, L. L., Mutti, P. R., Ferreira, R. F., Medeiros, S. S., Pérez-Marin, A. M., Marques, T., Ramos, T. M., de Lima Vieira, M. M., Oliveira, C. P., Gonçalves, W., Costa, G. B., Antonino, A., Menezes, R., Bezerra, B., & Santos e Silva, C. M. (2020). Seasonal variation in net ecosystem CO_2 exchange of a Brazilian seasonally dry tropical forest. *Scientific Reports*, *10*, 9454.

Moncrieff, G. R., Hickler, T., & Higgins, S. I. (2015). Intercontinental divergence in the climate envelope of major plant biomes. *Global Ecology and Biogeography*, *24*, 324–334.

Mooney, H., Medina, E., & Bullock, S. (1995). Neotropical deciduous forests. In E. Medina, H. A. Mooney, & S. H. Bullock (Eds.), *Seasonally dry tropical forests* (pp. 221–242). Cambridge University Press.

Muller-Landau, H. C., Cushman, K. C., Arroyo, E. E., Martinez Cano, I., Anderson-Teixeira, K. J., & Backiel, B. (2021). Patterns and mechanisms of spatial variation in tropical forest productivity, woody residence time, and biomass. *New Phytologist*, *229*, 3065–3087.

Murphy, P. G., & Lugo, A. E. (1986). Ecology of tropical dry forest. *Annual Review of Ecology and Systematics*, *17*, 67–88.

Nemani, R. R. (2003). Climate-driven increases in global terrestrial net primary production from 1982 to 1999. *Science*, *300*, 1560–1563.

Olson, D. M., Dinerstein, E., Wikramanayake, E. D., Burgess, N. D., Powell, G. V. N., Underwood, E. C., D'amico, J. A., Itoua, I., Strand, H. E., Morrison, J. C., Loucks, C. J., Allnutt, T. F., Ricketts, T. H., Kura, Y., Lamoreux, J. F., Wettengel, W. W., Hedao, P., & Kassem, K. R. (2001). Terrestrial ecoregions of the world: A new map of life on earth. *Bioscience*, *51*, 933–938.

Pan, N., Feng, X., Fu, B., Wang, S., Ji, F., & Pan, S. (2018). Increasing global vegetation browning hidden in overall vegetation greening: Insights from time-varying trends. *Remote Sensing of Environment*, *214*, 59–72.

Pennington, R. T., Lavin, M., & Oliveira-Filho, A. (2009). Woody plant diversity, evolution, and ecology in the tropics: Perspectives from seasonally dry tropical forests. *Annual Review of Ecology, Evolution and Systematics*, *40*, 437–457.

Portillo-Quintero, C., Sánchez-Azofeifa, A., Calvo-Alvarado, J., Quesada, M., & do Espirito Santo, M. M. (2015). The role of tropical dry forests for biodiversity, carbon and water conservation in the neotropics: Lessons learned and opportunities for its sustainable management. *Regional Environmental Change*, *15*, 1039–1049.

Poulter, B., Frank, D., Ciais, P., Myneni, R. B., Andela, N., Bi, J., Broquet, G., Canadell, J. G., Chevallier, F., Liu, Y. Y., Running, S. W., Sitch, S., & van der Werf, G. R. (2014). Contribution of semi-arid ecosystems to interannual variability of the global carbon cycle. *Nature*, *509*, 600–603.

R Core Team. (2019). Accessed September-25-2020, https://www.r-project.org/.

Ratnam, J., Tomlinson, K. W., Rasquinha, D. N., & Sankaran, M. (2016). Savannahs of Asia: Antiquity, biogeography, and an uncertain future. *Philosophical Transactions of the Royal Society B: Biological Sciences*, *371*, 20150305.

Rojas-Robles, N. E., Garatuza-Payán, J., Álvarez-Yépiz, J. C., Sánchez-Mej a, Z. M., Vargas, R., & Yépez, E. A. (2020). Environmental controls on carbon and water fluxes in an old-growth tropical dry forest. *Journal of Geophysical Research: Biogeosciences*, *125*, e2020JG005666.

Scheffer, M., Bascompte, J., Brock, W. A., Brovkin, V., Carpenter, S. R., Dakos, V., Held, H., Van Nes, E. H., Rietkerk, M., & Sugihara, G. (2009). Early-warning signals for critical transitions. *Nature*, *461*, 53–59.

Schlesinger, W. H., & Bernhardt, E. S. (2020). *Biogeochemistry: An analysis of global change* (4th ed.). Elsevier.

Schloss, A. L., Kicklighter, D. W., Kaduk, J., Wittenberg, U., & The participants of the Potsdam NPP Model Intercomparison. (1999). Comparing global models of terrestrial net primary productivity (NPP): Comparison of NPP to climate and the normalized difference vegetation index (NDVI). *Global Change Biology*, *5*(S1), 25–34.

Schwartz, N. B., Litner, B. R., Feng, X., & Powers, J. S. (2020). Beyond MAP: A guide to dimensions of rainfall variability for tropical ecology. *Biotropica*, *52*, 1319–1332.

Seddon, A. W. R., Macias-Fauria, M., Long, P. R., Benz, D., & Willis, K. J. (2016). Sensitivity of global terrestrial ecosystems to climate variability. *Nature*, *531*, 229–232.

Slik, J. W. F., Franklin, J., Arroyo-Rodr guez, V., Field, R., Aguilar, S., Aguirre, N., Ahumada, J., Aiba, S.-I., Alves, L. F., Avella, A. K. A., Mora, F., Aymard, G. A., Báez, S., Balvanera, P., Bastian, M. L., Bastin, J.-F., Bellingham, P. J., van den Berg, E., da Conceição Bispo, P., … Zang, R. (2018). Phylogenetic classification of the world's tropical forests. *Proceedings of the National Academy of Science of the USA*, *115*, 1837–1842.

Ssemmanda, I., Gelorini, V., & Verschuren, D. (2014). Sensitivity of east African savannah vegetation to historical moisture-balance variation. *Climate of the Past*, *10*, 2067–2080.

Stan, K., & Sánchez-Azofeifa, A. (2019). Tropical dry forest diversity, climatic response, and resilience in a changing climate. *Forests*, *10*, 443.

Stan, K. D., Sánchez-Azofeifa, A., Duran, S. M., Guzman, J. A., Hesketh, M., Laakso, K., & Dotterl, S. (2021). Tropical dry forest resilience and water use efficiency: An analysis of productivity under climate change. *Environmental Research Letters*, *16*, 054027.

Staver, A. C., Archibald, S., & Levin, S. A. (2011). The global extent and determinants of savanna and forest as alternative biome states. *Science*, *334*, 230–232.

Sullivan, M. J. P., Lewis, S. L., Affum-Baffoe, K., Castilho, C., Costa, F., Sánchez, A. C., Ewango, C. E. N., Hubau, W., Marimon, B., Monteagudo-Mendoza, A., Qie, L., Sonké, B., Martinez, R. V., Baker, T. R., Brienen, R. J. W., Feldpausch, T. R., Galbraith, D., Gloor, M., Malhi, Y., ..Phillips, O. L. (2020). Long-term thermal sensitivity of Earth's tropical forests. *Science*, *368*, 869–874.

Therneau, T., & Atkinson, B. (2019). *Recursive partitioning and regression trees*. https://cran.r-project.org/web/packages/rpart/index.html.

Vicente-Serrano, S. M., Gouveia, C., Camarero, J. J., Beguer a, S., Trigo, R., López-Moreno, J. I., Azor n-Molina, C., Pasho, E., Lorenzo-Lacruz, J., Revuelto, J., Morán-Tejeda, E., & Sánchez-Lorenzo, A. (2013). Response of vegetation to drought time-scales across global land biomes. *Proceedings of the National Academy of Science of the USA*, *110*, 52–57.

Walther, G.-R., Post, E., Convey, P., Menzel, A., Parmesan, C., Beebee, T. J. C., Fromentin, J.-M., Hoegh-Guldberg, O., & Bairlein, F. (2002). Ecological responses to recent climate change. *Nature*, *416*, 389–395.

Wang, B., Chen, G., & Liu, F. (2019). Diversity of the madden-Julian oscillation. *Science Advances*, *5*, eaax0220.

Winkler, K., Fuchs, R., Rounsevell, M., & Herold, M. (2021). Global land use changes are four times greater than previously estimated. *Nature Communications*, *12*, 2501.

Yu, F., Price, K. P., Ellis, J., & Shi, P. (2003). Response of seasonal vegetation development to climatic variations in eastern Central Asia. *Remote Sensing of Environment*, *87*, 42–54.

Zeng, F.-W., Collatz, G., Pinzon, J., & Ivanoff, A. (2013). Evaluating and quantifying the climate-driven interannual variability in global inventory modeling and mapping studies (GIMMS) normalized difference vegetation index (NDVI) at global scales. *Remote Sensing*, *5*, 3918–3950.

Zhang, C. (2005). Madden–Julian oscillation. *Reviews of Geophysics*, *43*, RG 2003.

Zhang, C. (2013). Madden–Julian oscillation: Bridging weather and climate. *Bulletin of the American Meteorological Society*, *94*, 1849–1870.

Zhang, Y., Xiao, X., Guanter, L., Zhou, S., Ciais, P., Joiner, J., Sitch, S., Wu, X., Nabel, J., Dong, J., Kato, E., Jain, A. K., Wiltshire, A., & Stocker, B. D. (2016). Precipitation and carbon-water coupling jointly control the interannual variability of global land gross primary production. *Scientific Reports*, *6*, 39748.

Zhao, M., & Running, S. W. (2010). Drought-induced reduction in global terrestrial net primary production from 2000 through 2009. *Science*, *329*, 940–943.

Zhou, L., Tian, Y., Myneni, R. B., Ciais, P., Saatchi, S., Liu, Y. Y., Piao, S., Chen, H., Vermote, E. F., Song, C., & Hwang, T. (2014). Widespread decline of Congo rainforest greenness in the past decade. *Nature*, *509*, 86–90.

Zhou, S., Yu, B., Huang, Y., & Wang, G. (2015). The complementary relationship and generation of the Budyko functions. *Geophysical Research Letters*, *42*, 1781–1790.

BIOSKETCH

Marinés de la Peña-Domene is interested in the conservation and restoration of tropical forests as a mitigation and adaptation strategy for climate change, particularly in agricultural contexts.

SUPPORTING INFORMATION

Additional supporting information can be found online in the Supporting Information section at the end of this article.

How to cite this article: de la Peña-Domene, M., Tapia, G. R., Mesa-Sierra, N., Rivero-Villar, A., Giardina, C. P., Johnson, N. G., & Campo, J. (2022). Climatic and edaphic-based predictors of normalized difference vegetation index in tropical dry landscapes: A pantropical analysis. *Global Ecology and Biogeography*, *31*, 1850–1863. https://doi.org/10.1111/geb.13565